

Temperature dependence of oxygen isotope acid fractionation for modern and fossil tooth enamels

Benjamin H. Passey*, Thure E. Cerling and Naomi E. Levin

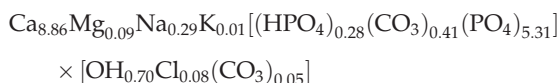
Department of Geology and Geophysics, University of Utah, 135 S. 1460 E. Rm 719, Salt Lake City, UT 84112, USA

Received 27 March 2007; Revised 19 June 2007; Accepted 20 June 2007

The oxygen isotope ratio of CO₂ liberated from structural carbonate in tooth enamel apatite was measured at phosphoric acid reaction temperatures of 25°C, 60°C and 90°C, and it was found that apparent acid fractionation factors for pristine enamel, fossilized enamel, and calcite follow different temperature relationships. Using sealed vessel reactions normalized to $\alpha_{25} = 1.01025$ (the fractionation factor for calcite at 25°C), the apparent fractionation factor at 90°C (α_{90}^*) for pristine enamel ranged between 1.00771 and 1.00820, and between 1.00695 and 1.00772 for fossilized enamel. Apparent fractionation factors for common acid bath reactions are similar to those for sealed vessel reactions. A significant correlation exists between α_{90}^* and F⁻ content, suggesting that change in the acid fractionation factor may be related to the replacement of OH⁻ with F⁻ during fossilization of bioapatite. These results have important implications for making accurate comparisons between modern and fossil tooth enamel $\delta^{18}\text{O}$ values, and for the uniformity of isotope data produced in different laboratories using different acid reaction temperatures. Copyright © 2007 John Wiley & Sons, Ltd.

The oxygen isotopic composition of vertebrate bioapatite is widely used for ecological and climatic reconstruction in modern and fossil settings.^{1–8} The oxygen isotope ratio of bone and tooth bioapatite is determined by that of body water, and this in turn is related to the weighted isotopic inputs and outputs of oxygen in the animal system.^{9,10} Empirical studies show a strong correlation between bioapatite $\delta^{18}\text{O}$ and meteoric water $\delta^{18}\text{O}$ values for certain species,^{2,6,11} and a strong humidity effect in others.^{5,6,12,13} There is also clear evidence that seasonal environmental signals are preserved as intra-tooth oxygen isotopic zoning,^{14,15} and the use of tooth enamel as a proxy for ancient seasonality is becoming increasingly common.^{16–18}

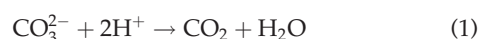
This study examines how the oxygen isotopic composition of CO₂ liberated by phosphoric acid digestion of the carbonate component of bioapatite varies as a function of acid temperature. Isotopic determination of bioapatite is routinely performed on either the phosphate or the carbonate component of the mineral, and these phases have been shown to be in isotopic equilibrium in pristine material.^{19–21} A recent approximation of the composition of bioapatite is:²²



Traditional determination of the phosphate component involves chemical isolation of phosphate from other oxygen-bearing phases in the mineral, followed by 100%

conversion of the phosphate oxygen into O₂ via fluorination.² This results in little or no isotopic fractionation between oxygen in the isotopically measured gas phase (O₂ or CO₂ produced by running the O₂ over hot graphite) and oxygen in the phosphate of the mineral phase. More recent approaches involve high-temperature reduction of phosphate to produce CO as the isotopic analyte; these do not typically involve 100% conversion of phosphate oxygen, and require calibration against standards on a run to run basis.³

Of relevance to this study, the isotopic analysis of the carbonate component of bioapatite involves acid digestion:



and partitioning of the carbonate oxygen into more than one phase. There is a resulting temperature-dependent isotopic fractionation between the measured gas phase (CO₂) and the carbonated mineral phase. For calcite, the CO₂ is approximately 10.3‰ enriched in ¹⁸O compared with the mineral when a 25°C reaction temperature is used, and this decreases to about 8.2‰ enrichment for a 90°C reaction temperature.^{23,24} Hydroxide in bioapatite may also play a role in modifying the isotopic composition of evolved CO₂ during acid digestion.

Despite the wide usage of oxygen isotope data from the carbonate component of bioapatite, no studies report the temperature-dependent acid fractionation, and workers have instead utilized acid fractionation factor-temperature relationships developed for calcite. For this study, we examined the temperature dependence of acid fractionation

*Correspondence to: B. H. Passey, Department of Geology and Geophysics, University of Utah, 135 S. 1460 E. Rm 719, Salt Lake City, UT 84112, USA.

E-mail: passey@earth.utah.edu

Contract/grant sponsor: University of Utah and National Science Foundation (USA).

for a suite of modern and fossil tooth enamels, for two sedimentary apatites, and for NBS-19 calcite.

EXPERIMENTAL

Four modern teeth and ten fossil teeth were studied. The modern teeth include Burchell's zebra (*Equus burchelli*), African elephant (*Loxodonta africana*), black rhino (*Diceros bicornis*), and hippo (*Hippopotamus amphibius*) molars collected in Kenya between 1998 and 2000. The fossil teeth include bison and camelid molars from the Rancho La Brea tar pits, California, USA (late Pleistocene), a proboscidean molar from Idaho, USA (Pliocene), hippo and proboscidean molars from Lothagam, Kenya (late Miocene), a proboscidean molar from Spain (Pliocene), and four equid molars from Nebraska, USA (late Miocene and Pliocene). The phosphate rock standards NBS-120c and NBS-694, and the calcite standard NBS-19, were also analyzed for comparison.

Tooth enamel was cut from teeth, and dentine, cementum, and surface-altered material were removed by grinding to leave a pure enamel sample. The samples were ground to powder using a ceramic mortar and pestle, and treated for 24 h in separate steps of 3% H₂O₂ and 0.1 M CH₃COOH. The samples were rinsed in double-distilled water between and after treatments, oven-dried at 60–70°C, and stored in a desiccator until needed for analysis. The samples were thoroughly mixed prior to analysis to maximize homogeneity.

The sealed vessel phosphoric acid reaction method generally follows that of McCrea.²⁵ Enamel powder (20–30 mg) was placed in one leg of a split 'two-legged man' vessel, and 4–5 mL 100% H₃PO₄ was placed in the other. The vessels were evacuated to a pressure of <10^{−4} Torr for at least 2 h, and the acid was heated under vacuum to drive off free water. The vessels were removed from the vacuum manifold and immersed in a temperature-controlled water bath, and the contents were reacted after sufficient time had elapsed to allow the sample and acid temperature to equilibrate with the bath temperature. Reactions were carried out at 25°C, 60°C and 90°C (±1°C) for durations of 48 h, 6 h and 3 h, respectively, unless noted otherwise. Following reaction, the CO₂ samples were extracted and purified using cryogenic methods, and sealed in Pyrex tubes containing several milligrams of silver wool. The silver wool was used as a precaution against possible SO₂ contamination.

The common acid bath method is a Finnigan Carboflo[®] split positive pressure/vacuum system (Bremen, Germany; now Thermo Scientific). Enamel samples (~500 µg) are reacted for 10 min in a rapidly stirring (turbulent) 100% H₃PO₄ bath (~5 mL) held at 90°C. Liberated CO₂ and H₂O are swept in a He stream (~60 mL/min) through ethanol/dry ice and liquid N₂ traps. Following the reaction period, the He flow is diverted and the liquid N₂ trap (with solid sample CO₂ inside) is evacuated. When sufficient vacuum is achieved (~10^{−3} Torr), the liquid N₂ is removed from the trap, and the sample CO₂ is cryogenically transferred to the micro-volume device in a Finnigan 252 isotope ratio mass spectrometer. Stable isotope analysis is performed using the dual inlet system, with the micro-volume

cold-finger held at −50°C to help prevent H₂O from entering the mass spectrometer source.

All sample sets were reacted and analyzed along with NBS-19 calcite, and the isotope values were normalized to this standard reacted at 25°C, using the accepted values of δ¹³C_{NBS-19} = 1.95‰ (PDB) and δ¹⁸O_{NBS-19} = −2.19‰ (PDB). When possible, precision was maximized for each tooth enamel standard by analyzing samples during the same extraction period and mass spectrometer run. The average precision achieved during a single run was 0.04‰ for δ¹³C and 0.06‰ for δ¹⁸O (1σ). For samples extracted and analyzed in different runs, the precision for tooth enamel using the sealed vessel method is closer to ~0.05% for δ¹³C and ~0.20‰ for δ¹⁸O when normalized to calcite standards.

Fluoride was determined by standard fluoride electrode potentiometry following the methods outlined by Bryant,²⁶ and the carbonate content was calculated for samples reacted using the sealed vessel method by measuring the CO₂ yield with a pressure gauge. The fluoride data are accurate and precise to about 10% of the reported numbers, whereas the CO₂ yield data are accurate to about 10%, and precise to about 5% of the reported numbers.

Apparent acid fractionation factors α^{*}_T were calculated using the following equation:²⁴

$$\alpha_T^* = \frac{\left(\frac{\delta^{18}\text{O}_T}{1000} + 1\right) \times \alpha_{25}}{\frac{\delta^{18}\text{O}_{25^\circ\text{C}}}{1000} + 1} \quad (2)$$

where α₂₅ is the acid fractionation factor for calcite at 25°C (=1.01025; refs^{23,27}), α^{*}_T is the acid fractionation factor of the unknown sample at the temperature of interest, and δ¹⁸O_{25°C} and δ¹⁸O_T are the oxygen isotopic compositions of CO₂ evolved from reactions of the unknown samples at 25°C and the temperature of interest, respectively.

No attempt was made to determine absolute fractionation factors for bioapatite; this would require direct isotopic analysis of carbonate using a method where all carbonate oxygen is converted into the measured gas phase, with no contamination from other oxygen-bearing phases, so that there is no isotopic fractionation between the mineral carbonate phase and the measured gas phase. No such method currently exists, and the feasibility of such a method is uncertain. Instead, we follow the approach used by Swart *et al.*,²⁴ and assign the acid fractionation factor at 25°C to be equal to the value determined for calcite by earlier studies. This allows for normalization of data and calculation of 'apparent' fractionation factors at other temperatures using Eqn. (2).

RESULTS

Results for sealed vessel analyses are shown in Table 1 and Fig. 1. Modern teeth have α^{*}_T values slightly lower than calcite, with α^{*}₆₀ = 1.00889 ± 0.00015 and α^{*}₉₀ = 1.00791 ± 0.0002 for the four modern samples. The calcite standard NBS-19 gives α^{*}₉₀ = 1.00818 ± 0.00002, similar to the values reported by Swart *et al.*²⁴ for two different calcites (1.00821 and 1.00827). The following equation describes the

Table 1. Isotope ratios and fractionation factors as a function of acid temperature for sealed vessel reactions

T (°C)	Reaction time (min)	n	CO ₂ yield (1σ) μmol/mg	δ ¹³ C (1σ) ‰, PDB	δ ¹⁸ O (1σ) ‰, PDB	α* (std. error)
<i>K98-326-LAI – modern horse – Kenya</i>						
25	2880	2	0.59 (0.02)	0.30 (0.01)	1.95 (0.04)	1.01025
60	360	3	0.60 (0.02)	0.30 (0.01)	0.53 (0.04)	1.00882 (0.00006)
90	180	2	0.62 (0.00)	0.26 (0.02)	-0.28 (0.04)	1.00800 (0.00006)
<i>AMBO-25 – modern elephant – Kenya</i>						
25	2880	2	0.72 (0.00)	-6.38 (0.01)	-0.70 (0.02)	1.01025
60	360	3	0.73 (0.00)	-6.37 (0.01)	-2.09 (0.07)	1.00884 (0.00007)
90	180	3	0.76 (0.00)	-6.40 (0.04)	-3.21 (0.14)	1.00771 (0.00014)
<i>K00-AB-303 – modern rhino – Kenya</i>						
25	2880	3	0.50 (0.00)	-12.88 (0.02)	-0.86 (0.03)	1.01025
60	360	2	0.58 (0.01)	-12.84 (0.05)	-2.07 (0.09)	1.00903 (0.00009)
90	180	2	0.60 (0.00)	-12.87 (0.01)	-2.89 (0.02)	1.00820 (0.00004)
<i>K00-AS-165 – modern hippo – Kenya</i>						
25	3900	3	0.56 (0.00)	-1.94 (0.03)	-2.82 (0.08)	1.01025
60	360	3	0.61 (0.01)	-1.92 (0.01)	-4.19 (0.02)	1.00887 (0.00008)
90	180	3	0.63 (0.01)	-2.05 (0.07)	-5.31 (0.10)	1.00773 (0.00013)
<i>LACM HC 59211 – fossil bison – California – Rancho La Brea</i>						
25	660	3	0.59 (0.06)	-2.40 (0.04)	-3.21 (0.06)	1.01025
60	120	3	0.64 (0.01)	-2.31 (0.04)	-4.66 (0.06)	1.00878 (0.00008)
90	60	3	0.70 (0.01)	-2.26 (0.02)	-5.53 (0.02)	1.00790 (0.00006)
<i>LACM HC 1066 – fossil camelid – California – Rancho La Brea</i>						
25	2880	3	0.76 (0.01)	-5.47 (0.05)	-2.53 (0.02)	1.01025
60	360	2	0.81 (0.01)	-5.39 (0.03)	-3.95 (0.03)	1.00881 (0.00004)
90	180	3	0.84 (0.01)	-5.37 (0.06)	-4.68 (0.03)	1.00806 (0.00004)
<i>ID STD – fossil proboscidean – Idaho – Pliocene</i>						
25	2880	3	0.62 (0.07)	-11.26 (0.05)	-10.68 (0.12)	1.01025
60	360	2	0.66 (0.01)	-11.22 (0.01)	-12.64 (0.04)	1.00826 (0.00013)
90	180	2	0.71 (0.00)	-11.21 (0.01)	-13.73 (0.06)	1.00714 (0.00014)
<i>LOTH-122 – fossil hippo – Kenya – Lothagam – Miocene</i>						
25	2880	3	0.69 (0.01)	-6.03 (0.01)	-5.70 (0.07)	1.01025
60	360	3	0.69 (0.01)	-6.00 (0.02)	-7.61 (0.05)	1.00831 (0.00009)
90	180	2	0.71 (0.01)	-6.01 (0.01)	-8.78 (0.07)	1.00712 (0.00009)
<i>LOTH-64 – fossil proboscidean – Kenya – Lothagam – Miocene</i>						
25	2880	5	0.77 (0.01)	-1.70 (0.04)	0.53 (0.02)	1.01025
90	120	4	0.82 (0.01)	-1.64 (0.06)	-2.74 (0.22)	1.00695 (0.00022)
<i>SP STD – fossil proboscidean – Spain – Pliocene</i>						
25	3900	4	0.49 (0.03)	-10.95 (0.01)	-3.01 (0.04)	1.01025
60	360	2	0.49 (0.00)	-10.95 (0.01)	-4.81 (0.07)	1.00843 (0.00008)
90	180	2	0.54 (0.00)	-10.92 (0.01)	-5.71 (0.02)	1.00751 (0.00004)
<i>UNSM – fossil horses – 4 different individuals – Nebraska – Mio/Pliocene</i>						
90	120	4	-	-	-	1.00772 (0.0012)
<i>SRM-120c – phosphate rock reference material</i>						
25	2820	3	0.65 (0.01)	-6.27 (0.04)	-1.13 (0.05)	1.01025
90	120	3	0.70 (0.01)	-6.24 (0.04)	-3.62 (0.17)	1.00773 (0.00018)
<i>SRM-694 – phosphate rock reference material</i>						
25	2820	3	0.30 (0.00)	-9.32 (0.02)	-6.07 (0.06)	1.01025
90	120	3	0.39 (0.02)	-9.33 (0.03)	-9.56 (0.04)	1.00670 (0.00007)
<i>NBS-19 – calcite reference material</i>						
25	540	2	7.90 (0.3)	1.95 (0.01)	-2.19 (0.02)	1.01025
90	240	2	10.35 (0.2)	1.94 (0.01)	-4.23 (0.01)	1.00818 (0.00002)

temperature relationship for modern tooth enamel, with temperature in °K:

$$\alpha_T^* = 1.00312(\pm 0.00026) + \frac{635(\pm 27)}{T^2} \quad (3)$$

Fossil tooth enamel shows a greater amount of variability in α_T^* . The late Pleistocene Rancho La Brea tar pit samples are indistinguishable from the modern samples, with the two samples giving $\alpha_{60}^* = 1.00880 \pm 0.00009$ and $\alpha_{90}^* = 1.00798 \pm 0.00007$. Three of the fossil samples, ID STD, LOTH-122, and LOTH-64, have significantly lower values, averaging $\alpha_{60}^* = 1.00828 \pm 0.00013$ and $\alpha_{90}^* = 1.00707 \pm 0.00025$, while a fourth, SP STD, has intermediate values

of $\alpha_{60}^* = 1.00843 \pm 0.0008$ and $\alpha_{90}^* = 1.00751 \pm 0.00004$. The UNSM fossil horse samples have an α_{90}^* value of 1.00772 ± 0.00012 that is similar to the values for two of the modern teeth, AMBO-25 and K00-AS-165. The following equation describes the temperature relationship for fossil tooth enamel (excluding the Rancho La Brea data):

$$\alpha_T^* = 1.00112(\pm 0.00036) + \frac{809(\pm 38)}{T^2} \quad (4)$$

The phosphate rock materials differ from each other in α_{90}^* , with NBS-120c giving a value of 1.0077 ± 0.00018 , and NBS-694 giving a value of 1.00670.

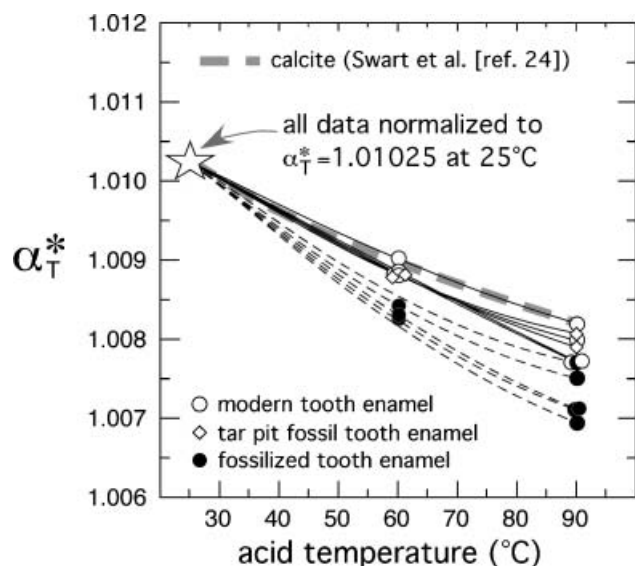


Figure 1. Apparent fractionation factors as a function of acid temperature for different types of tooth enamel. All data are for sealed vessel reactions. The relationship for calcite is shown for reference (thick dashed gray line; Swart *et al.*²⁴). The thin solid and dashed lines connect identical samples reacted at different temperatures.

Results for common acid bath analyses are shown in Table 2 and Fig. 2. Common acid bath α_{90}^* values track sealed vessel α_{90}^* values, without statistically significant offset in either direction. There is a fairly good correlation between common acid bath and sealed vessel α_{90}^* values ($R^2 = 0.80$; Fig. 2), and the regression slope is significantly different from zero ($p = 0.006$), and not significantly different from 1 ($p > 0.4$).

As expected, carbon isotope ratios show no relationship with temperature, with the exception of the two Rancho La Brea tar pit samples, which become ~ 0.10 to 0.15% enriched in ^{13}C between 25°C and 90°C . This may result from the differential release and modification of hydrocarbons in

these samples at different temperatures and for different reaction times.

Fluoride data are given in Table 2 and are plotted with α_{90}^* data in Fig. 3. The fluoride concentration in modern tooth enamel is low and ranges between about 70 and 370 ppm. The Rancho La Brea tar pit samples, LACM HC 92411 and 1066, have F^- concentrations of about 150 and 280 ppm, respectively, indistinguishable from the modern teeth. The other fossil tooth enamel has elevated F^- , ranging from about 3500 ppm (UNSM 1132-93) to 14 000 ppm (EA STD), and the phosphate rock materials have concentrations in excess of 30 000 ppm (SRM-120c is certified at 38 200 ppm, and SRM-694 at 32 000 ppm). Linear regression for α_{90}^* as the dependent variable and F^- as the independent variable shows significant correlation between the two variables ($R^2 = 0.80$), and gives a slope that is different than zero at $>95\%$ confidence ($p = 0.0005$; Fig. 3).

CO_2 yields are given in Table 1, and average carbonate content data are given in Table 2. There is no significant difference in carbonate content between modern and fossil enamel (t-test, $p = 0.28$), and no correlation between carbonate content and acid fractionation factor ($R^2 = 0.11$, $p = 0.39$). The CO_2 yields typically increase as reaction temperature increases, such that 90°C reactions have 0–10% higher yields than 25°C reactions (Table 1). This presumably relates to the efficiency of CO_2 removal from the viscous acid during gas extraction, and the observation of bubbles forming in the acid during extractions performed at lower temperatures supports this idea. It is unlikely that this effect has a large influence on the acid fractionation factor data: carbon isotope variation as a function reaction temperature is typically $<0.1\%$, indicating that isotope effects resulting from incomplete acid degassing are negligible. In addition, we observe 90°C calcite fractionations that are indistinguishable from those reported in the literature, despite lower CO_2 extraction efficiencies at 25°C compared to 90°C . Finally, acid fractionation factors are similar for SV and CAB reactions, despite very different CO_2 extraction mechanisms between these (passive degassing under vacuum in the former, and active degassing in the latter resulting from turbulent stirring of the acid, and continuous purging with helium).

Table 2. Common acid bath (CAB) acid fractionation factors (90°C), fluoride content, and carbonate content

Sample ID	n (CAB)	α_{90}^* CAB (std. error)	ppm F^- (std. error)	wt % CO_3 (1σ)
K98-326-LAI	2	1.00759 (0.00004)	67 (7)	3.6 (0.1)
AMBO-25	3	1.00788 (0.00005)	182 (20)	4.4 (0.1)
K00-AB-303	2	1.00803 (0.00005)	368 (50)	3.3 (0.3)
K00-AS-165	2	1.00778 (0.00013)	–	3.5 (0.2)
LACM HC 59211	–	–	150 (15)	4.0 (0.2)
LACM HC 1066	–	–	280 (40)	4.8 (0.2)
ID STD	–	–	8014 (1700)	4.1 (0.2)
LOTH-122	3	1.00713 (0.00008)	5680 (540)	4.2 (0.1)
LOTH-64	3	1.00646 (0.00005)	13900 (1400)	4.8 (0.2)
SP STD	3	1.00734 (0.00006)	4780 (500)	3.0 (0.2)
UNSM 1132-93	–	–	3450 (400)	4.1 (0.1)
NBS-19	2	1.00819 (0.00001)	–	60.2 (2.5)
SRM 120c	–	–	38200 ^a	4.0 (0.2)
SRM 694	–	–	32000 ^a	2.1 (0.4)

^a NIST certified.

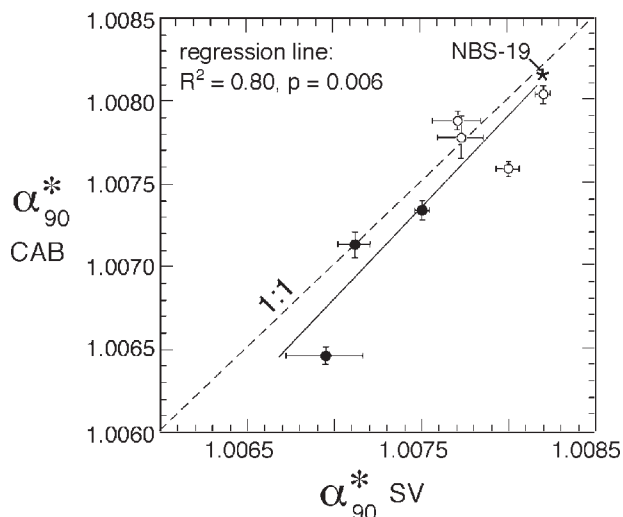


Figure 2. Common acid bath (CAB) apparent fractionation factors versus sealed vessel (SV) apparent fractionation factors for reactions at 90°C. Black circles are fossil enamel, and open circles are modern enamel. Results for NBS-19 calcite (star) are shown for reference. Dashed line is the 1:1 relationship, and solid line is the least-squares linear regression (excluding NBS-19 data).

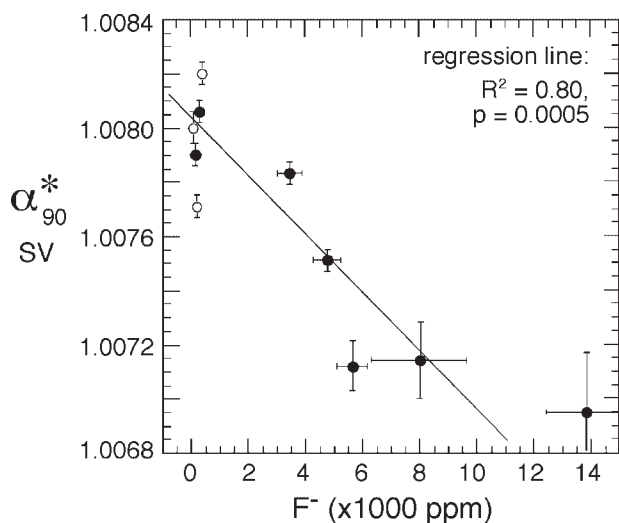


Figure 3. Sealed vessel apparent fractionation factor at 90°C plotted versus F^- content for several modern and fossil enamels (data from Tables 1 and 2). Black circles are fossil enamel, and open circles are modern enamel.

DISCUSSION

Implications for reproducibility of carbonate oxygen isotope data

The results from this study clearly show that acid fractionation factors developed for calcite are not always applicable to tooth enamel bioapatite. Fossil enamels, in particular, may have α^*_T temperature dependencies that differ significantly from those of calcite, and the use of calcite fractionation factors may result in up to 1–1.5‰ discrepancies in reported $\delta^{18}\text{O}$ data when very different reaction temperatures are used (Fig. 4). On the other hand, some of the modern enamel bioapatites have α^*_T temperature dependencies that are practically indistinguishable from

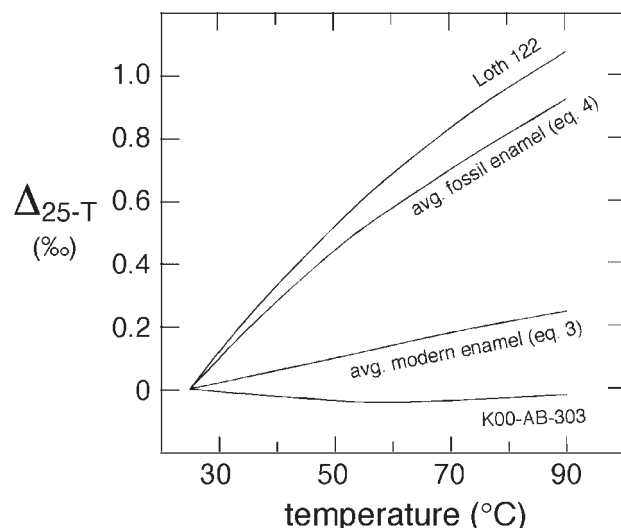


Figure 4. Expected difference in $\delta^{18}\text{O}$ values between samples reacted at 25°C and samples reacted at other temperatures when calcite fractionation factors are used to normalize data. $\Delta_{25-T} = \delta^{18}\text{O}(25^\circ\text{C}) - \delta^{18}\text{O}(T^\circ\text{C})$, i.e., Δ_{25-T} is the per mil difference in $\delta^{18}\text{O}$ between a sample reacted at 25°C and the same sample reacted at another temperature. $\delta^{18}\text{O}$ values for enamels with fractionation factor temperature relationships similar to calcite (K00-AB-303) will be affected less than those for enamels with very different temperature relationships (LOTH-122).

those of calcite, and there will be little difference in reported $\delta^{18}\text{O}$ data for laboratories analyzing samples at different temperatures. Virtually all published bioapatite $\delta^{18}\text{O}$ values have been reported using calcite acid fractionation factors, and this must be taken into account, especially when comparing data for fossil enamel generated at different temperatures.

This study also shows that there is a significant amount of variation in α^*_T within the categories of modern and fossil enamel. For α^*_{90} , modern enamel has a range of about 0.5‰, and fossil enamel has a range of about 1.1‰. In addition, although α^*_{90} values for common acid bath reactions compare well with values for sealed vessel reactions (Fig. 2), they typically are not exactly equivalent to these, and there is an average absolute difference of 0.2‰ (max = 0.5‰, min = 0.01‰). These results are perhaps not surprising since, compared with calcite and other carbonate minerals, bioapatite is a highly variable mineral that allows for a variety of chemical substitutions. Variability in α^*_T values may be a manifestation of this chemical variability, and this may impose real limitations on the level of reproducibility for data generated using different phosphoric acid reaction techniques at different temperatures. As thoroughly discussed by Swart *et al.*,²⁴ different reaction methods and temperatures will involve different effective exchange times between CO_2 and acid (or water in acid), and different degrees of dissolution of CO_2 into acid, and efficiency of CO_2 removal from acid. Inasmuch as these factors appear to affect α^*_T values for calcite, they may also be expected to have a significant effect on values for bioapatite.

Use of fractionation factors defined by Eqns. (3) and (4) for modern and fossil enamels, respectively, will help to reduce

inconsistencies in reported $\delta^{18}\text{O}$ values from laboratories analyzing samples at different temperatures. However, because there is variability in α^*_T values for different modern and fossil enamels, these equations cannot be assumed to be valid for any particular enamel sample. When different analytical methods are used (e.g., GasBench, Kiel-type, common acid bath, and sealed vessel reactions) and a high degree of reproducibility is required, it may be necessary to investigate α^*_T temperature patterns for materials representative of each sample suite.

The relationship between α^*_T and F^- content

Two commonly observed changes in fossil tooth enamel compared with modern tooth enamel are an increase in F^- content^{28–30} and a decrease in the oxygen isotopic difference between phosphate and structural carbonate^{29–32} (though increases have been observed for some samples³¹). This study shows that there is also a change in the temperature dependence of acid fractionation. In this section we address the correlation observed between α^*_T and fluoride content (Fig. 3), and highlight the possibility that removal of OH^- during fossilization may influence α^*_T values. It should be appreciated, however, that correlation does not prove causality, and that the following line of reasoning is sufficient but not necessary to explain the observed changes in α^*_T .

Because oxygen is exchangeable between CO_2 and H_2O , and because OH^- will rapidly convert into H_2O in the presence of acid, it may be reasonable to expect that changes in the OH^- content of bioapatite will influence the oxygen isotope ratio of acid-liberated CO_2 . It has been shown that there is some (albeit minor) oxygen exchange between CO_2 and H_2O present in strong H_3PO_4 solutions.³³ The influence on the oxygen isotopic composition of CO_2 by H_2O produced during the reaction is unknown, but the direction and magnitude of equilibrium fractionation between these phases (+41‰ at 25°C) suggests that CO_2 will become enriched in ^{18}O as the relative amount of reaction-produced H_2O increases.²³ However, this will occur only to the extent that H_2O is not rapidly and effectively removed from the system by absorption into the hydroscopic acid phosphate compounds in '100%' phosphoric acid, and to the extent that the CO_2 - H_2O oxygen exchange approximates closed-system behavior.

Apatite minerals include fluorapatite, ideally $\text{Ca}_5(\text{PO}_4)_3\text{F}$, and hydroxyapatite, ideally $\text{Ca}_5(\text{PO}_4)_3\text{OH}$, and there is a solid solution between these phases. Preservation of charge balance upon uptake of F^- in apatites probably involves removal of OH^- . If the F^- content of bioapatite increases at the expense of OH^- , then the regression shown in Fig. 3 is consistent with the idea that the acid fractionation-temperature slope changes with changing OH^- content. Also consistent with this line of reasoning is the fact that the Rancho La Brea tar pit material is 'fossil' enamel but has F^- and α^*_T patterns similar to modern enamel. Therefore, the observed correlation between α^*_T and F^- supports the idea that α^*_T is sensitive to the OH^- content of bioapatite, and that changes in OH^- content lead to changes in α^*_T .

Is there an expected direction in which the $\delta^{18}\text{O}$ value of CO_2 liberated from bioapatite should move with

progressive loss of OH^- ? Unfortunately, the oxygen isotopic spacing between CO_3^{2-} and OH^- in tooth enamel is unknown, as is the degree of isotopic alteration of the remaining OH^- (and CO_3^{2-} occupying the OH^- site) when OH^- is replaced by F^- . Furthermore, the direction and magnitude of fractionation between CO_2 , OH^- , and reaction-produced H_2O during acid dissolution of bioapatite carbonate are unknown and are likely to be temperature-dependent. Kohn *et al.*²⁹ took similar uncertainties into account and predicted a change of -1.5% to $+1\%$ in the isotopic composition of the bulk mineral for loss of all OH^- . As for the CO_3^{2-} component and acid-liberated CO_2 , there is no predictable direction in which the oxygen isotopic composition should change with loss of OH^- .

The correlation between α^*_{90} and F^- is good but not perfect (Fig. 2). For example, there is a significant range in α^*_{90} for modern tooth enamel (about 0.5‰) that is not mirrored by differences in F^- content, and the carbonate fluorapatite reference materials SRM 120c and SRM 694 have very different sealed vessel α^*_{90} values (1.00773 vs. 1.00670) despite having similar F^- concentrations. Therefore, there are probably other factors that contribute to the measured value of α^*_T . Diagenetic alteration of bioapatite, including changes in CO_3^{2-} distribution and content,^{34,35} uptake of foreign elements and inclusion of oxyhydroxides,²⁹ and changes in mineral structure³⁶ cannot be ruled out as factors possibly influencing α^*_T .

A decrease in acid fractionation during fossilization may also account for part of the decreased oxygen isotopic spacing between carbonate and phosphate observed in fossil bioapatite, but this study does not address that possibility because the measured fractionation factors are 'apparent' and not absolute. That is to say, this study shows that there is a difference in the α_T versus temperature slope between modern and fossil enamel, but for any particular temperature it does not indicate the direction or absolute magnitude of change in acid fractionation.

CONCLUSIONS

The results presented in this paper show that the temperature dependence of acid fractionation in the carbonate component of enamel bioapatite is not the same as that of calcite, as had previously been assumed. Isotopic discrepancies of the order of 0 to 1.5‰ are expected between laboratories analyzing fossil tooth enamel at different temperatures when calcite fractionation factors have been used, and discrepancies of 0 to 0.5‰ are expected for modern tooth enamel. Use of enamel-specific fractionation factors will help improve the analytical reproducibility between different laboratories. However, there is significant variability in α^*_T for different enamels within the categories of modern and fossil enamel, and this imposes limitations on inter-lab reproducibility when analyzing samples with unknown α^*_T temperature relationships. Fortunately, the expected error that this might impose does not greatly exceed that of other analytical approaches, and is within the level of accuracy needed for meaningful application to many questions.

Acknowledgements

We thank Jim Ehleringer, Craig Cook, and Mike Lott for provision of the SIRFER mass spectrometry facility, and the University of Utah and National Science Foundation (USA) for funding.

REFERENCES

- Land LS, Lundelius EL, Valastro S. *Palaeogeogr. Palaeoclim. Palaeoecol.* 1980; **32**: 143.
- Longinelli A. *Geochim. Cosmochim. Acta* 1984; **48**: 385.
- Vennemann TW, Fricke HC, Blake RE, O'Neil JR, Colman A. *Chem. Geol.* 2002; **185**: 321.
- Koch PL, Behrensmeier AK, Tuross N, Fogel ML. *Carnegie Institute of Washington Yearbook.* 1990; 105.
- Ayliffe L, Chivas AR. *Geochim. Cosmochim. Acta* 1990; **54**: 2603.
- Huertas AD, Iacumin P, Stenni B, Sanchez Chillón B, Longinelli A. *Geochim. Cosmochim. Acta* 1995; **59**: 4299.
- Koch PL. *Annu. Rev. Earth Planet. Sci.* 1998; **26**: 573.
- Kohn MJ, Cerling TE. *Rev. Mineral. Geochem.* 2002; **48**: 455.
- Bryant JD, Froelich PN. *Geochim. Cosmochim. Acta* 1995; **59**: 4523.
- Kohn MJ, Schoeninger M, Valley J. *Geochim. Cosmochim. Acta* 1996; **60**: 3889.
- Iacumin P, Longinelli A. *Earth Planet. Sci. Lett.* 2002; **201**: 213.
- Luz B, Cormie AB, Schwarcz HP. *Geochim. Cosmochim. Acta* 1990; **54**: 1723.
- Levin NE, Cerling TE, Passey BH, Harris JM, Ehleringer JR. *Proc. Natl. Acad. Sci. USA* 2006; **103**: 11201.
- Koch PL, Fisher DC, Dettman DL. *Geology* 1989; **17**: 515.
- Fricke HC, O'Neil JR. *Palaeogeog. Palaeoclim. Palaeoecol.* 1996; **126**: 91.
- Kohn MJ, Miselis JL, Fremd TJ. *Earth Planet. Sci. Lett.* 2002; **204**: 151.
- Zazzo A, Mariotti A, Lecuyer C, Heintz E. *Palaeogeog. Palaeoclim. Palaeoecol.* 2002; **186**: 145.
- Balasse M, Ambrose SH, Smith AB, Price TD. *J. Arch. Sci.* 2002; **29**: 917.
- Iacumin P, Bocherens H, Mariotti A, Longinelli A. *Earth Planet. Sci. Lett.* 1996; **142**: 1.
- Bryant JD, Koch PL, Froelich PN, Showers WJ, Genna BJ. *Geochim. Cosmochim. Acta* 1996; **60**: 5145.
- Vennemann TW, Hegner E, Cliff G, Benz GW. *Geochim. Cosmochim. Acta* 2001; **65**: 1583.
- Elliott JC. *Rev. Mineral. Geochem.* 2002; **48**: 427.
- Friedmann I, O'Neil JR. *U.S. Geological Survey Professional Paper* 1977; **440-KK**.
- Swart PK, Burns SJ, Leder JJ. *Chem. Geol. (Isot. Geosci. Sect.)* 1991; **86**: 89.
- McCrea JM. *J. Chem. Phys.* 1950; **18**: 849.
- Bryant JD. *Oxygen isotope systematics in body water and in modern and fossil equid tooth enamel phosphate*, PhD thesis, Columbia University, 1995; 256.
- Sharma T, Clayton RN. *Geochim. Cosmochim. Acta* 1965; **29**: 1347.
- Bryant JD, Froelich PN, Showers WJ, Genna BJ. *Palaios* 1996; **11**: 397.
- Kohn MJ, Schoeninger MJ, Barker WW. *Geochim. Cosmochim. Acta* 1999; **63**: 2737.
- Fox DL, Fisher DC. *Palaios* 2001; **16**: 279.
- Showers WJ, Barrick R, Genna B. *Anal. Chem.* 2002; **74**: 142A.
- Fricke HC, Clyde WC, O'Neil JR, Gingerich PD. *Earth Planet. Sci. Lett.* 1998; **160**: 193.
- Wachter EA, Hayes JM. *Chem. Geol. (Isot. Geosci. Sect.)* 1985; **52**: 365.
- Sponheimer M, Lee-Thorp JA. *J. Arch. Sci.* 1999; **26**: 143.
- Zazzo A, Lecuyer C, Sheppard SMF, Grandjean P, Mariotti A. *Geochim. Cosmochim. Acta* 2004; **68**: 2245.
- Michel V, Ildefonse P, Morin G. *Appl. Geochem.* 1995; **10**: 145.